UDC 537.525.5; 533.924; 621.793.1

N.N.Koval[1,2], Yu.F.Ivanov[1,2], O.V.Krysina[1], V.V.Shugurov[1,2], I.V.Lopatin[1]

[1]*Institute of High Current Electronics SB RAS;*
[2]*National Research Tomsk Polytechnic University, Russia*

# Synthesis of multicomponent nanocrystalline coatings based on titanium nitride in arc low-pressure discharges

The paper considers peculiarities of ion-plasma equipment and treatment of materials in vacuum arc discharges. The advantages and the prospects of the modified ion plasma setup used for coating deposition are described. The parameters of generated arc gas and gas-metal plasma were measured and presented. Dependences of metal material surface properties on gas-discharge plasma parameters are revealed. Vacuum arc plasma-assisted deposition of multicomponent nanocrystalline coatings based on titanium nitride is presented. The effect of added elements on the structural phase state and characteristics of titanium nitride-based coatings is demonstrated.

*Key words:* arc discharge, ion plasma setup, vacuum arc deposition, plasma assistance, plasma parameters, nanocrystalline coating, titanium nitride.



## *Introduction*

At present, multicomponent functional coatings are obtained by various physical vapor deposition methods: magnetron sputtering [1, 2], vacuum arc deposition [3, 4], hybrid methods [5, 6] with simultaneous use of ion sources, magnetrons, electric arc evaporators, etc. Researchers involved with coating synthesis also supplement deposition equipment with various devices to increase the efficiency of deposition or minimize its shortcomings, e.g., with gas discharge or metal ion plasma sources, electron guns, independent heating and cooling systems of substrates, bias voltage supplies, plasma filters, plasma optics or focusing systems, cathodes of various designs or complex composition [7–11], etc.

Modification and improvement of related equipment and technology makes possible multicomponent nanocrystalline coatings with unique physicomechanical and service properties: super- and ultrahardness 40–100 GPa, low friction coefficient <0.2, high degree of elastic recovery 80–94 %, elastic strain >10 %, high rupture strength 10–40 GPa [12], and high thermal stability up to 1700ºC [13].

In the work, multicomponent nanocrystalline coatings were synthesized by vacuum arc plasma-assisted deposition in which the metal component of the plasma is formed on evaporation of the cathode material from cathode spots of an arc discharge and ionized reactive gas (nitrogen) is supplied to the working zone. This method offers the following significant advantages over other methods: (1) wide operating pressure range ($10^{-1}$ … $10^{-4}$ Pa); (2) high ionization degree (20–100 %); (3) possibility to use almost all metals, alloys, and composites as the cathode material; and (4) high coating growth rate (~10 μm/h) [14]. For increasing the characteristics of deposited coatings, the available ion plasma setup was equipped with a gas discharge plasma source, a bias voltage supply operating in steady and pulsed modes, an electric arc evaporator with enhanced cathode cooling, composite cathodes of complex composition, etc.

In the paper investigations of the operating parameters of the modified vacuum arc setup, research of parameters of generated gas, metal and gas-metal plasma, synthesis of multipurpose nanocrystalline coatings with high physicomechanical properties, and examination of these properties are considered.

## *Equipment and its peculiarities*

In experiments, a TRIO automated vacuum ion plasma setup (Fig. 1) was used to study the generation of dense low-temperature plasma on vacuum arc evaporation of cathodes of complex composition and the plasma parameters for synthesis of multicomponent nanocrystalline coatings. The main units of the setup are a modified DI-100 electric arc evaporator with enhanced cathode cooling, a standard NNV6-I1 electric arc evaporator, an original PINK filament plasma source [15, 16], and a bias voltage supply operating in both steady and pulsed modes. For the evaporated cathode material we used sintered Ti-Cu, Ti-Al, and Ti-Si composites made at the Institute of Strength Physics and Materials Science SB RAS [17].

The modifications of the deposition setup made it possible to considerably increase the efficiency of ion plasma cleaning and activation of substrate surfaces, nitriding of steels and alloys, and electric arc plasma-assisted synthesis of functional coatings in a single vacuum cycle.


*a)* *b)*

Figure 1. View of ion-plasma setup «TRIO» (a) and power supply unit with PC control (b)

First, the modified electric arc evaporator DI-100 (Fig. 2) allowed more efficient generation of metal arc plasma compared to widely used arc evaporators of NNV-6 and Bulat setups; namely, a change in the cathode unit design made it possible to increase the cooled cathode surface area from 28 % (NNV-6) and 30 % (Bulat) to 80 %, thereby greatly decreasing its integral temperature during vacuum arc evaporation. As a result, the droplet fraction in the plasma flow was decreased. For example, in Ti coating deposition with a standard NNV-6 electric arc evaporator at an arc current of 100 A and deposition time of 10 min, the volume fraction of macroparticles in the coating is about two times larger than that ensured with the DI-100 evaporator at the same parameters. The average droplet size in both cases is almost the same and is 0.7 μm. As the DI-100 evaporator was changed for the NNV-6 evaporator, the amount of macroparticles increased 2–3 times.

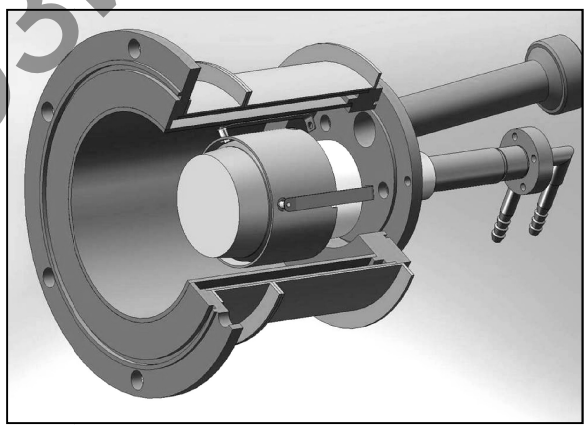

Figure 2. Model of modified arc evaporator DI-100

One more design peculiarity of the DI-100 arc evaporator is the possibility to employ evaporated cathodes made of porous materials (e.g., silumin or materials obtained by self-propagating high-temperature synthesis (SHS)), which is impossible with standard arc evaporators. Besides, a copper diaphragm of thickness

0.5 mm is placed between the evaporated cathode and its water cooling system, ensuring rather efficient cooling and precluding direct contact of cooling water with the cathode.

It should be noted that the DI-100 source is intended for use in industrial technological processes of coating synthesis: the diameter of the working cathode is 100 mm and its height is $h$ = 50–60 mm, i.e., the volume of the working cathode material is 2–4 times larger than that for NNV-6 and Bulat setups; the maximum discharge current is increased to 250 A making possible a coating growth rate up to 20 μm/h. Fig. 3 shows the growth rate distribution of a TiN coating for the standard and modified arc evaporators along the axis of the chamber located 300 mm away from the cathode surface. It is seen that within the plasma spread angle, the deposition uniformity varies but slightly (15–20 %) for both arc evaporators; however, the average coating growth rate for the DI-100 evaporator is 1.5–2 times higher than that for the standard NNV-6 plasma source.

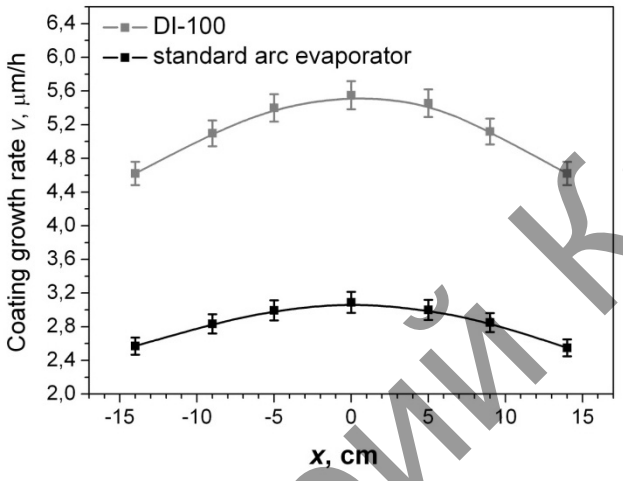


Figure 3. Growth rate distribution of a TiN coating along the axis of the vacuum chamber for a standard evaporator (NNV-6) and modified DI-100 arc evaporator (100 A, rotation, $U_b = U_{fl}$)

The second distinctive feature of vacuum arc deposition in the work is the use of Ti-based composite cathodes, e.g., Ti-Cu, Ti-Al, Ti-Si, Ti-Cr, etc. These cathodes are obtained by SHS or vacuum sintering of powders. The use of composite cathodes provides mixed plasma as such rather than plasma flow of several simultaneously evaporated single-element cathodes. Unlike mosaic cathodes, in which the base material is embedded with inclusions of another material, composite cathodes do not reveal any long local immobility of cathode spots. In our early works, it was shown that the characteristics of Ti-based cathodes with a low addition concentration (≤15 at. %), in particular Ti-Cu and Ti-Si systems, are similar to or higher than those of VT1-0 titanium cathodes traditionally used in synthesis of titanium nitride coatings [18, 19]:

1. The erosion rates for cathodes made of Ti-Cu and Ti-Si with an addition concentration up to 15 at. % and VT1-0 alloy cathode at a discharge current $I_d$ = 50–100 A are equal within the error and are ≈50–55μg/C;
2. The growth rate of nitride coatings in evaporation of composite materials with a low concentration of added elements and titanium cathode is the same and is ≈1.5 μm/h at a discharge current $I_d$ = 50 A and ≈3.0 μm/h at a discharge current $I_d$ = 100 A;
3. The characteristics of cathode spots for composite cathodes and titanium alloy cathode, such as the average cathode spot velocity, average current per spot, and number of spots at a certain discharge current, are close. (With Ti-Si cathodes, the cathode spot velocity is 1.5–2 times higher than that with a titanium cathode, suggesting that the droplet fraction in the plasma is smaller);
4. Composite cathodes are uniformly evaporated with no dominant erosion of one of structural components (the average crater diameter is $d_{av}$ ≈ 100 μm; the grain size of the main material phases of a composite cathode is 3–20 μm);
5. The droplet fraction for Ti-Cu composite cathodes with a low Cu concentration and for a Ti cathode is characterized as follows: the area occupied by droplets with Ti-12 at. % Cu is 1.5 times larger than that with Ti; the average droplet diameter is 0.8 (Ti) and 0.9 μm (Ti-12 at. % Cu); the total amount of droplets from the Ti cathode is 10 % larger than that from the composite cathode.

The next improvement of vacuum arc surface treatment and deposition of wear-resistant coatings on materials and articles is the use of a plasma source based on a low-pressure non-self-sustained arc discharge (PINK). The plasma generator has the following parameters:

– high arc discharge currents with no cathode spot ($I_d$ up to 250 A);
– low operating pressure ($p = 10^{-2}$–$10^{-1}$ Pa);
– high ion current density ($j_s$ up to 10 mA/cm$^2$) at a plasma density $n = 10^{10}$–$10^{11}$ cm$^{-3}$;
– reasonably high uniformity (± 5–10 %) in large volumes (~0.1 m$^3$).

Supply of ionized working gas and appropriate negative bias potential applied to a substrate allows easy control of the ion energy delivered to the specimen and thus the following ion plasma processes:

1. Finishing surface cleaning and activation of specimens in the plasma of inert gas at low operating pressures.

Notice that for the gas discharge plasma produced at low operating pressures ($10^{-2}$–$10^{-1}$ Pa), the mean free path of an ion increases and is larger than the characteristic size of the space charge layer formed near a substrate to which negative bias is applied. As the negative bias is varied, the ions that arrive on the substrate surface after transit through the space charge layer formed near the substrate at low pressures are accelerated to an energy corresponding to the applied potential, because the energy loss in collision with other particles can be neglected. Thus, gas ions of energy ~100–1000 eV allow cleaning of a thin surface layer (oxide films, adsorbed gases) of specimens with little change of their initial structure, and their heating and activation for further ion plasma treatment (nitriding, coating deposition).

2. Nitriding of steels and alloys in the nitrogen plasma of a non-self-sustained arc discharge with a filament and hollow cathode.

Ion-plasma nitriding of steels and alloys with the PINK generator has several advantages over conventional methods:

– nitriding at decreased temperatures (200–550 ºC), making possible treatment of steels with a low tempering temperature;
– possibility to apply negative bias voltage to treated substrates (> 150 V) to increase the nitriding efficiency;
– continuous low-energy ion bombardment with removal of oxides that retard nitrogen diffusion deep into specimens;
– reduction of the nitriding time 2–5 times compared to conventional nitriding methods;
– possibility to obtain a modified layer of thickness reaching 300 μm, depending on nitriding conditions and substrate composition [20, 21];
– use of only commercially pure nitrogen as the working gas.

3. Plasma-assisted synthesis of coatings.

The PINK source is efficient in magnetron and vacuum arc plasma-assisted deposition of coatings. First, deposition at low pressures (~10–1 Pa) makes possible coatings almost free of gas atoms, i.e., with a more dense structure. Second, continuous low-energy ion bombardment of a growing coating ensures removal of adsorbed gas from the surface and refinement of the coating structure. Third, additional ions produced by the PINK source and present in the volume of the vacuum chamber provides stable ignition of a cold-cathode arc discharge at low currents (<20 A). Fourth, the use of the plasma source in combination with a system of negative bias voltage supply ensures a considerable decrease in droplet phase fraction, which is a grave shortcoming of vacuum arc deposition. The decrease in droplet fraction in this mixed (metal and gas) low-pressure arc discharge plasma owes to reflection of macroparticles negatively charged to the floating potential (between –6 and –8 V) in the arc discharge plasma (Te ≈ 5–7 eV) from a treated specimen which is at a negative potential (about –100 V) [22, 23].

The next peculiarity of the modified equipment and, hence, of the coating deposition method is the use of a negative bias supply operating in pulsed and steady modes. In the pulsed mode, its main parameters are a negative bias voltage $U_b$ of 0–1000 V, duty factor τ of 10–90 %, and pulse repetition frequency $f$ of 10–50 kHz.

A distinguishing feature of the pulsed mode of bias supply is a several-fold increase in ion current to a substrate during the pulse rise time. The authors of [24] demonstrated that at –300 V, the ion current amplitude to a substrate increases 1.5–3 times when switching from the steady to pulsed mode, depending on the

pulse repetition frequency. Notice that as the voltage pulse amplitude is increased, the ion current does not reach saturation, as opposed to the steady mode, and increases proportionally to the pulse amplitude and frequency; and the higher the pulse repletion frequency, the higher the rate of rise of the ion current with an increase in pulse amplitude [25]. The increase in ion current involves appropriate variation in the plasma properties: the electron temperature and ionization degree of the working gas increases [25].

The pulsed mode of bias supply provides the possibility to:

– preliminary clean substrates from oxide films and adsorbed gases with no breakdown and hence with no damage to the surface of treated substrates;

– apply bias to dielectric substrates and films during deposition.

This owes to compensation of the positive space charge on the specimen surface (dielectric or dielectric inclusion) by the electron flow during the pulse-to-pulse interval in a time no longer than 5 μs [26]. Efficient compensation requires frequencies above 1 kHz [26]. One more positive effect of negative bias voltage in coating synthesis is a wide parameter control range which makes possible various structural phase states and hence various physicomechanical characteristics of coatings.

*The use of gas plasma of the arc discharge for ion-plasma etching of materials surface*

Ion-plasma treatment of samples surface in low-pressure plasma based on non-self-sustained arc discharge can be applied to ion-plasma etching of a surface, as a preliminary stage of synthesis of functional coatings or as an independent stage of finishing treatment of materials and products surface. Due to etch removal of a thin surface layer by gas ions the samples cleaning from oxide films and the adsorbed gases, heating of a sample (T~100ºC) and surface activation occur.

Further the complex research of gas plasma of arc low-pressure discharges, surfaces of metal samples after ion-plasma etching at different modes of arc discharge; identification of a dependence chain (characteristic of discharge burning modes) → (plasma parameters) → (properties of surface layer) are considered.

For carrying out processes of ion-plasma etching the plasma generated by non-self-sustained arc low-pressure discharge with the combined filament and hollow cathode «PINK» [15, 16] was used.

For research of plasma the single cylindrical probe and the unique automated system of probe measurements of plasma parameters [27] was used. It provides rather small time of the probe characteristic measurement (~ 1 min), high accuracy and quality of measurements (± 0,1% on voltage channel, ± 0,5% on the current channel, ADC capacity – 14 bits), reliability of measurements and simplicity of operation. The probe was situated directly on an axis of a plasma source at distance of 450 mm from its output aperture. For each chosen mode the probe characteristic was measured. The floating potential, the plasma potential and temperature of electrons were determined by a graphic method. The plasma concentration was calculated in terms of electronic branch of the probe voltage-current characteristic.

Measurements of plasma parameters based on non-self-sustained arc discharge with the combined hollow cathode and filament, and also cleaning and etching of samples surface were carried out in argon with a pressure of ~0,1 Pa. Samples were fixed on rotating tool in the center of the working camera. The substrates were made of stainless steel 12Cr18Ni10Ti and a hard alloy of WC-8%Co. The substrates before ion-plasma treatment were mechanically polished to a roughness of $R_a$ = 0,07 μ*m* and cleaned in an ultrasonic bath in gasoline and alcohol. For measurement of etching rate the glass mask was fixed on a sample surface before ion-plasma treatment. Etching rate of a material was calculated in terms of height of the formed step.

All samples were preliminary etched by argon ion for cleaning of their surface within 20 min at arc current of $I_P$ = 20 A and negative pulsed (γ = 50 %) bias of $U_b$ = -200 V. After that there was no considerable etching of a surface which could affect values of measured characteristics. After preliminary treatment the samples were exposed to ion-plasma etching at the main mode. The changeable parameters were the value of bias (200÷1000 V) and arc discharge current (10÷90 A). Duration of ion-plasma treatment was 60 min for all samples.

The substrates after ion-plasma treatment were investigated by means of hardness tester of PMT-3 (microhardness), optical micro-nano-profilometer MNP-1 (roughness, thickness of removed layer), metalgraphic microscope μVizo-MET-221 (surface image, structure), scanning electron microscope Philips SEM-515 (surface image, structure).

Typical images of sample surface of alloy WC-Co and stainless steel 12Cr18Ni10Ti after ion-plasma treatment are given in Fig. 4. In Fig. 4 (a) typical etching of cobalt binding on grain boundary of tungsten carbides of an alloy WC-Co is visible. In Fig. 4 (b) the area of etched step of steel material is presented. On the left there is the area which was behind a mask; on the right the area which has undergone ion-plasma bombardment is visible.

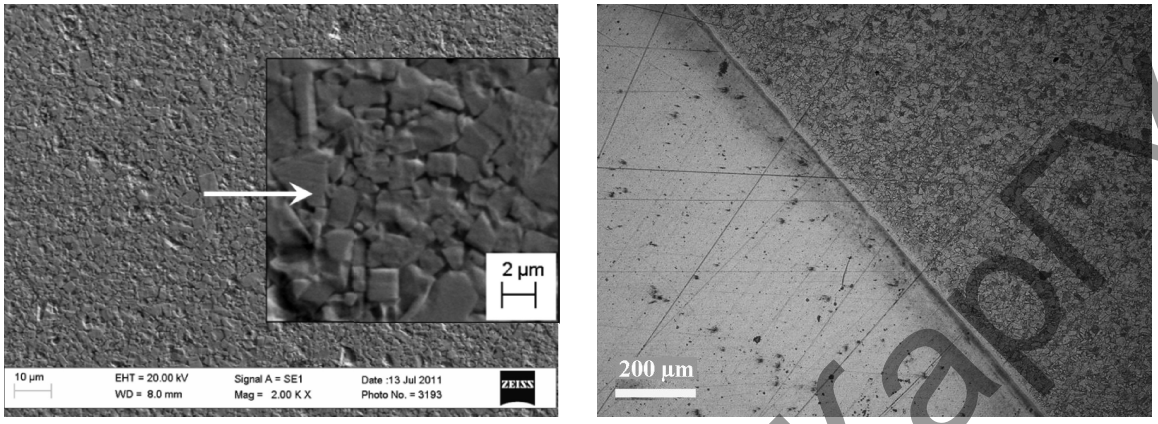


*a)* *b)*

Figure 4. Typical SEM image of alloy WC-Co surface (a) and the image of a steel surface in the field of a step (b), obtained by optical microscope after treatment in plasma of arc discharge (Ar; 0,3 Pa; 20 A; -1000 V)

Plasma parameters in dependence on the chosen modes of arc discharge at which sample surface was treated are given in Table 1. At increase of filament current, and, respectively, current of electron emission from hot cathode, the growth of arc discharge current of «PINK» occurs and changes of discharge voltage. That, in turn, leads to increase of gas plasma concentration. It was established that the growth of arc discharge current from 10 A to 90 A leads to increase of concentration of argon plasma from $0{,}3 \cdot 10^{16}$ to $5{,}2 \cdot 10^{16}$ $m^{-3}$. In the conditions the potential of plasma has a positive sign concerning the anode and increases from 5,4 to 6,4 V. Temperature of electrons in all range of discharge currents changes slightly, and its average value is ≈1,4 eV.

Table 1

**Plasma parameters against parameters of the arc discharge: filament current ($I_f$), discharge current ($I_P$), discharge voltage ($U_d$), plasma potential ($U_{pl}$), temperature of electrons ($T_e$), concentration of plasma ($n$)**

| $I_f$, A | $I_P$, A | $U_d$, V | $U_{pl}$, V | $T_e$, eV | $n$, $\times 10^{16}$, $m^{-3}$ |
|---|---|---|---|---|---|
| 117 | 10 | 59 | 5,5 | 1,4 | 0,3 |
| 129 | 20 | 58 | 5,4 | 1,6 | 1,0 |
| 154 | 50 | 55 | 5,7 | 1,3 | 2,7 |
| 187 | 90 | 50 | 6,4 | 1,3 | 5,2 |

The investigation of samples after treatment at a constant bias voltage and at increase of arc discharge current, i.e. at increase of plasma concentration and ion current density on the substrate (Table 1, 2) showed that the roughness of steel substrate doesn't change, but etching rate at increase of discharge current changes slightly. For a substrate of hard alloy the roughness of a surface increases in proportion to arc discharge current. In the case there is cobalt binding loss, and the grains of tungsten carbide «become bare». Etching rate at arc discharge current <50 A don't change and remains equal to ≈0,4 µ*m*/*h*. At increase of arc discharge current up to 90 A the etching rate increases in ≈2 times. That can be explained by sufficient density of ion current and ion energy for etching of tungsten carbide at these parameters of treatment. But it should be taken into account that the accuracy of definition of step height in the case is lower, than in case of lower arc discharge current because of a higher roughness of treated surface.

Table 2

**Characteristics of samples surface of steel 12Cr18Ni10Ti and WC-8%Co alloy after ion-plasma etching *vs.* parameters of treatment mode ($v_e$ — etching rate, $T$ — substrate temperature, $j_s$ — ion current density on substrate)**

| $I_P$, $A$ | $j_s$, mA/cm$^2$ | $T$, ºC | 12Cr18Ni10Ti steel | | WC-8%Co | |
|---|---|---|---|---|---|---|
| | | | $v_e$, μm/$h$ | $R_a$, μm | $v_e$, μm/h | $R_a$, μm |
| 20 | 1,5 | 140 | 0,26 | 0,15 | 0,41 | 0,22 |
| 50 | 1,8 | 214 | 0,36 | 0,12 | 0,45 | 0,34 |
| 90 | 2,0 | 315 | 0,38 | 0,16 | 0,89 | 0,62 |

The properties of surface layer of treated samples are given in the Table 3 at change of substrate potential. It is clear that the roughness of steel samples practically doesn't change at increase of bias voltage to substrate. The etching rate increases at growth of negative bias voltage and reaches 0,64 μm/h at $U_b$ = -1000 V.

Table 3

**Characteristics of surface of 12Cr18Ni10Ti steel and WC-8%Co hard-alloy samples after ion-plasma etching against to parameters of treatment mode**

| $U_b$, V | $j_s$, mA/cm$^2$ | T, ºC | 12Cr18Ni10Ti steel | | WC-8%Co | |
|---|---|---|---|---|---|---|
| | | | $v_e$, μm/h | $R_a$, μm | $v_e$, μm/h | $R_a$, μm |
| 200 | 0,5 | 55 | - | 0,13 | - | 0,14 |
| 400 | 1,0 | 75 | - | 0,13 | - | 0,22 |
| 600 | 1,5 | 140 | 0,26 | 0,15 | 0,41 | 0,22 |
| 1000 | 2,5 | 232 | 0,64 | 0,14 | 0,58 | 0,34 |

For hard-alloy samples the similar tendency is observed. At increase of bias voltage the etching rate increases. But the surface roughness of hard-alloy samples increases at growth of substrate potential in contrast to steel samples (tab. 3).

It should be noted that the increase of arc current and also the increase of negative bias voltage leads to increase of ion current, and accordingly to increase of substrates temperature (see tab. 2, 3). That can be affects to etching rate of material.

Thus, by variation such parameters as arc current of plasma source «PINK» and substrate potential we can regulate concentration of plasma, ion current density on substrate, energy of ions arriving to substrate. That allows to etch the surface layers of a material with demanded thickness and to obtain necessary characteristics of its surface.

*Investigation of gas-metal plasma of arc low-pressure discharges, which are applied for synthesis of coatings by vacuum-arc deposition with plasma assistance*

Nature of plasmochemical reactions on a substrate, properties, the chemical composition and structure of deposited coatings are substantially defined by the processes which occur in interelectrode gap of a vacuum arc. Therefore research of plasma parameters, which is used for coatings deposition, is important. In the work the method of the vacuum-arc plasma-assisted deposition is used and the main object of researches is the gas-metal plasma generated by arc low-pressure discharges.

Below investigations of parameters of the plasma generated at independent and joint work of metal plasma source (arc evaporator) and gas-discharge plasma source («PINK») [15, 16] and identification of influence of plasma assistance on parameters of the mixed arc plasma, which is used for deposition of nitride coatings are given.

For research of plasma the single cylindrical Langmuir probe and the unique automated system for probe measurements of plasma parameters [27] was used. The probe is situated in the vacuum camera center directly on crossing of axes of plasma sources, at distance of 450 mm from an output aperture of «PINK» and at distance of 300 mm from an output aperture of the arc evaporator.

For each chosen mode the probe characteristic was fixed. The floating potential and plasma potential were determined by a graphic method. Temperature of electrons was defined from the probe characteristic in half-logarithmic scale. The plasma concentration was calculated from electronic branch of the probe voltage-current characteristic.

The pressure of working gas (argon, nitrogen) was p ≈ 0,3 Pa at all chosen modes. The arc discharge current of «PINK» at probe measurements of gas ($I_P$ = 10÷50 A) and gas-metal plasma ($I_P$ = 10÷90 A) was variable parameter. Research of metal and gas-metal plasma was carried out at arc currents of the evaporator ($I_d$) 50 and 100 A.

Average temperature of electrons in case of gas-discharge plasma was ≈1,4 eV, in case of the mixed gas-metal plasma — 0,9-1,0 eV. Potential and concentration of plasma in the case of the use of plasma source of «PINK» only in the nitrogen atmosphere increase in proportion to growth of arc discharge current (Fig. 5 (a)): from 3,3 to 4,2 V and from $0{,}2\cdot10^{16}$ to $2{,}0\cdot10^{16}$ $m^{-3}$, respectively. In the case of metal plasma at arc current of $I_d$ = 50 A (Fig. 5) without «PINK» use the concentration of plasma was $n = 2{,}2\cdot10^{16}$ $m^{-3}$ and plasma potential was equal to $U_{pl}$ = 2,4 V.

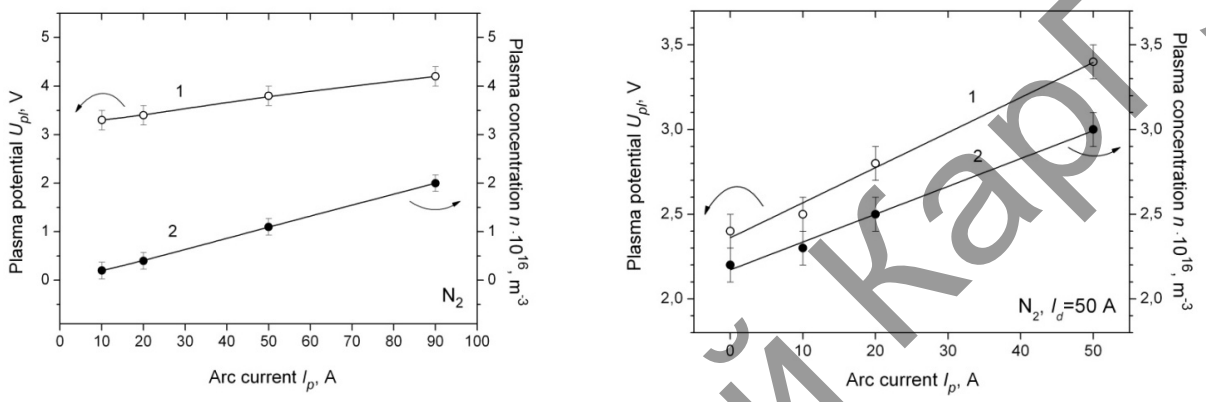


*a)* *b)*

(a) — nitrogen plasma; (b) — gas-metal plasma ($N_2$; $I_d$ = 50 A)

Figure 5. Dependence of plasma potential (1) and plasma concentration (2) on arc current of «PINK»

At arc current of $I_d$ = 100 A the metal plasma concentration increases ≈2 times (Fig. 6) in comparison with $I_d$ = 50 A and is equal to $n = 3{,}8\cdot10^{16}$ $m^{-3}$; plasma potential is $U_{pl}$ = 3,0 V. At simultaneous work of metal and gas-discharge plasma sources at $I_d$ = 50 A and growth of arc current of «PINK» from 10 to 50 A the plasma potential increases from 2,3 to 3,0 V (Fig. 5). The concentration of the gas-metal plasma increases at growth of arc current of «PINK» from $2{,}5\cdot10^{16}$ to $3{,}4\cdot10^{16}$ $m^{-3}$ at constant current of the arc evaporator. It is clear that these values correspond to the sum of concentration of gas-discharge plasma at a certain arc current of «PINK» and metal plasma without «PINK» use. The similar tendency is observed for arc current of $I_d$ = 100 A (Fig. 6).

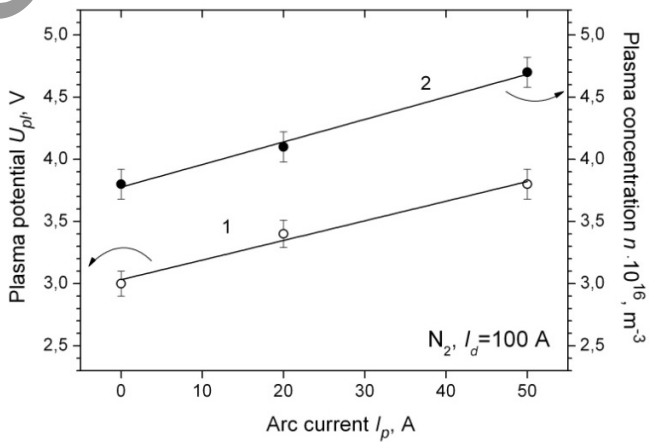


Figure 6. Dependence of potential of gas-metal plasma (1) and its concentration (2) on arc current of «PINK» ($N_2$; $I_d$ = 100 A)

For the mixed (gas-metal) plasma in the nonreactive argon atmosphere (Fig. 7, 8) similar dependences of plasma potential and concentration on arc current of «PINK» are observed at arc currents of the arc evaporator of 50 and 100 A. As in the case of nitrogen atmosphere, compliance of concentration of the mixed plasma to the sum of concentration for argon and metal plasma remains.

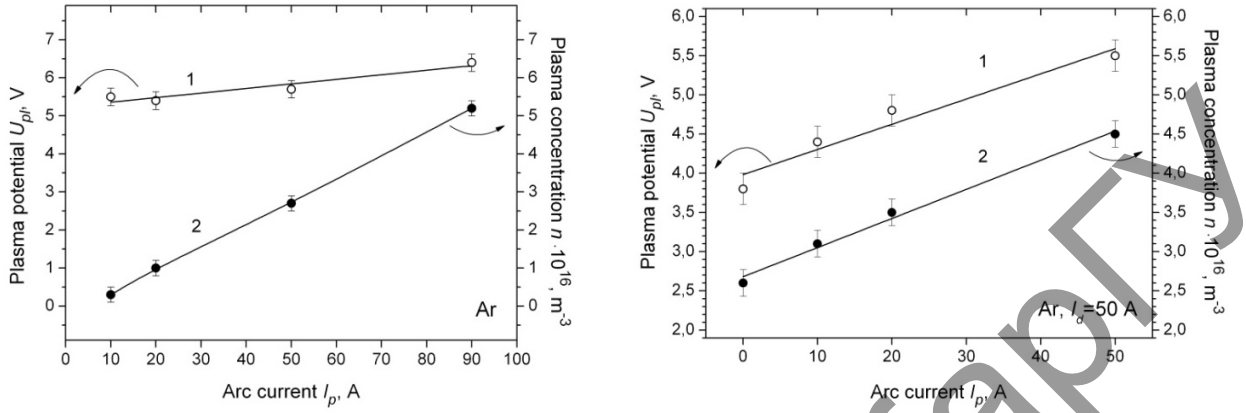


(a) — argon plasma; (b) — gas-metal plasma (Ar; $I_d$ = 50 A)

Figure 7. Dependence of plasma potential (1) and plasma concentration (2) on arc current of «PINK»

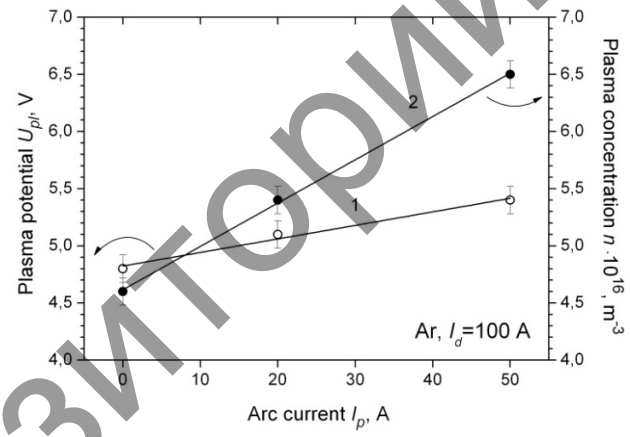


Figure 8. Dependence of potential of gas-metal plasma (1) and its concentration (2) on arc current of «PINK» (Ar; $I_d$ = 100 A)

It is shown that concentration of gas-metal plasma is approximately equal to the sum of concentration of the gas and metal plasma measured at similar parameters of arc discharges.

It was experimentally shown that the increase of arc current of «PINK» at constant pressure of working gas leads to increase of plasma concentration.

In case of simultaneous use of metal and gas-discharge plasma sources the growth of arc current of "PINK" at constant arc current of evaporator leads to the similar growth of gas-metal plasma concentration. The fact shows that by changing arc current of «PINK» (with constant pressure) at deposition of coatings we can easily regulate the ions current density of working gas on a substrate, thereby changing the stoichiometry of growing coatings. It will allow to simplify technology of deposition of multilayered and gradient coatings, and also to improve repeatability of deposition process for above types of coatings.

*Synthesis of coatings*

The substrate material was WC-8%Co hard alloy and 12Cr18Ni10Ti stainless steel. Before deposition, the specimens were mechanically polished with diamond paste to a roughness $R_a \sim 0.02$ μm, whereupon they were washed in an ultrasonic bath with gasoline and alcohol for 10 min and immediately placed in the vacu-

um chamber. The residual pressure ensured by a turbomolecular pump was ~$10^{-3}$ Pa. Directly before coating deposition, the specimen surface was cleaned from oxide films and absorbed gases through its bombardment by accelerated Ar ions at a negative substrate potential of ≈1 kV. The ion bombardment activated a surface layer of the substrates to provide high adhesion of the coating and substrate, and the specimens were heated up to ~300–400 °C. The formation of a nitride coating was preceded by condensation of a transition layer of thickness ~100 nm of the cathode material in the Ar plasma. With Ti-Cu, Ti-Al, and Ti-Si composite cathodes, multicomponent nitride coatings were deposited in the environment of commercially pure nitrogen at an arc discharge current $I_d$ = 50–100 A, working gas pressure $p_{N2}$ ~ 0.1 Pa, and bias voltage $U_b$ = –(100–300) V. The coating growth rate was 0.5–3 μm/h depending on deposition parameters and evaporated cathode material. The deposition time was chosen such that the coating thickness was ≈3 μm.

The properties of the deposited coatings were studied with the following equipment: a scanning electron microscope equipped with an elemental microanalyzer, a transmission electron microscope, an X-ray diffractometer, micro- and nano-hardness testers, a film and coating thickness gauge (Calotest), a high-temperature tribometer, and a 3D contactless profilometer.

*Properties and structure of nitride multicomponent coatings*

Table 4 presents measurements results for the following physicomechanical characteristics of the coatings: hardness (*HV*), Young's modulus (*E*), residual strain ($\varepsilon_{min}$), friction coefficient ($\mu_{min}$), concentration of added elements (*n*) determined by energy dispersive analysis and *X*-ray fluorescence analysis, and average crystallite size in the main phase ($d_{av}$).

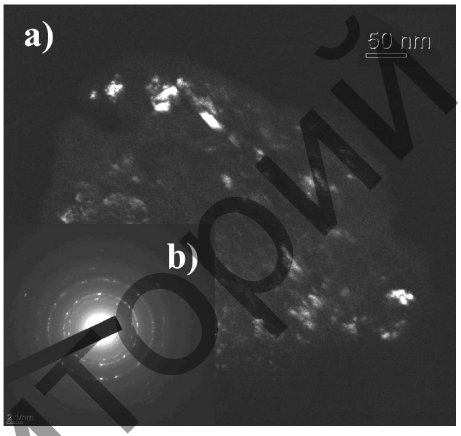


Figure 9. Electron micrograph of the Ti-Si-N coating structure: dark field in the {111} ring reflection of TiN (a) and electron diffraction pattern (b)

All three-component coatings have a nanocrystalline structure (Fig. 9). The main phase in all cases is δ-TiN; the average crystallite size is < 20 nm. The concentration of added elements in the coating and evaporated cathode is the same if the addition is Cu, Al. In the Ti-Si-N coatings, the Si concentration is five times lower than that in the cathode.

The multicomponent nanocrystalline coatings have a hardness ~1.5–2.5 times higher than the hardness of TiN coatings, and under optimum deposition conditions, the coatings are ranked as superhard (≥ 40 GPa). The highest residual strain is observed in the TiN coating; the least residual strain, in the Ti-Si-N coating. The elastic recovery for the coatings formed by evaporation of powder cathodes is 2–3 times higher than that in the TiN coating.

Table 4

**Characteristics of the coatings deposited by vacuum arc evaporation of composite cathodes of various compositions**

| Cathode composition | *n*, at.% | | $d_{av}$, nm (TEM) | *HV*, GPa | *E*, GPa | $\varepsilon_{min}$, % | $\mu_{min}$ |
|---|---|---|---|---|---|---|---|
| | (EDA) | (XFA) | | | | | |
| Ti | - | - | ~100 | 20-25 | 300-350 | ≈75 | 0.40 |
| Ti-12at.%Cu | ≈2 | ≈12 | 18 | 38-42 | 350-400 | ≈50 | 0.22 |
| Ti-10at.%Si | - | ≈2 | 7 | 34-52 | 400-800 | ≈20 | 0.41 |
| Ti-40at.%Al | ≈20 | - | 5-6 | 31-40 | 450-650 | ≈35 | 0.23 |

The elastic (Young's) modulus of the multicomponent coatings is in the range 350–800 GPa. The least friction coefficient is displayed by the coatings added with copper and aluminum; its value decreases down to 0.2 and points to an increase in the wear resistant of these coatings.

*Conclusion*

The studies on the modified setup show that all introduced modifications hold promise for application in ion plasma processes: surface cleaning and activation of substrates before deposition, ion plasma nitriding, and plasma-assisted synthesis of multicomponent nanocrystalline coatings. The parameters of generated gas and gas-metal plasma were measured and presented. Dependences of material surface properties on gas-discharge plasma parameters are revealed. The examination of the coatings made it possible to disclose the effect of added elements on the structural characteristics, phase and elemental composition, and physicomechanical properties of the Ti-Cu-N, Ti-Al-N, and Ti-Si-N coatings synthesized by vacuum arc plasma-assisted deposition.

*The work was partly supported by RFBR under Grant No. 11-08-00625-a, 12-08-31192_mol-a, 13-08-98108 r_sibir_a.*

References

1 Musil J., Vlcek J. // *Surface and Coatings Technology*, 112, 1999, p. 162–169.

2 Veprek S. et al. // *Thin solid Films* 476, 2005, p. 1–29.

3 Martin P.J. et al. // *Surface and Coatings Technology* 200, 2005, p. 2228–2235.

4 Flink A. et al. // *Surface & Coatings Technology* 200, 2005, p. 1535–1542.

5 Hyun S. Myung et al. // *Surface and Coatings Technology* 163–164, 2003, p. 591–596.

6 Martin P.J. et al. // *Surface and Coatings Technology* 163–164, 2003, p. 245–250.

7 Andre Anders. // *Vacuum* 67, 2002, p. 673–686.

8 Shulaev V.M. et al., *PSE*, 2008, vol. 6, No. 1–2, p. 4–19.

9 Ribeiro E. et al. // *Surface and Coatings Technology* 151–152, 2002, p. 515–520.

10 Shulaev V.M. et al., *PSE*, 2007, vol. 5, No. 1–2, p. 94–97.

11 Shtanskyy D.V., Kiryukhancev-Korneev F.V. et al. // *Fizika tverdogo tela*, 2005, vol. 47, No. 2, p. 242–251.

12 *Nanostructured coatings*, Albano Cavaleiro and Jeff Th.M De Hosson, Eds. Springer Science+Business Media, LLC, 2006.

13 Zeman P., Capek J., Cerstvy R., Vlcek J. // *Thin Solid Films* 519, 2010, p. 306–311.

14 Barvinok V.A., Bogdanovich V.I. *Physical Grounds and Mathematical Simulation of Ion-Plasma Evaporation*, Moscow: Mashinostroenie, 1999.

15 Borisov D.P., Schanin P.M., Koval N.N. // *Izv. Vuzov. Physika*, vol. 37, No. 3, 1994, p. 115–121.

16 Vintizenko L.G., Grigoriev S.V., Koval N.N., Tolkachev V.S., Lopatin I.V., Schanin P.M. *Hollow-cathode low-pressure arc discharges and their application in plasma generators and charged-particle sources* // Russian Physics Journal, 2001, vol. 44, No. 9, p. 927–936.

17 Pribytkov G.A., Savitskii A.P., Korosteleva E.N. // *Izv. Vuzov. Phyzika*, 2006, No. 8, p. 466–469.

18 Pribitkov G.A., Korostelyeva E.N. et al. // *Proceedings: VII Int. Conf. on Modification of Materials with Particle Beams and Plasma Flows*, Tomsk, Russia, July, 25–29, 2004, p. 167–170.

19 Krysina O.V. // *Proceeding of IV Russian conference of young scientists «Material science, technology and ecology in third century»* (19–21, october, 2009, Tomsk: IOA SB RAS, p. 229–232.

20 Schanin P.M. et al. *Phisika i khimija obrabotki materialov*, 2001, No. 3, p. 16–19.

21 Korotaev A.D. et al. *Phisika i khimija obrabotki materialov*, 2004, No. 1, p. 22–27.

22 Schanin P.M. et al. // *J. Tech. Phys.* (2000), vol. 41, No. 2, Special Issue, p. 177–184.

23 Schanin P.M. et al. // *In Proceedings: 1st International Congress on Radiation Physics, High Current Electronics and Modification of Materials*, Tomsk, Russia, 2000, vol. 3, p. 438–441.

24 Berlin E.V., Seydman L.A. *Ion-plasma processes in thin-film technology*, Moscow: Tekhnosphera, 2010.

25 Kelly P.J. et al. // *Surface and Coating Technology*, 142–144, — 2001, p. 635–641.

26 Barnat E. and Lu T.-M. // J. Vac. Sci. Technol. A., 1999, vol. 17, No. 6, p. 3322–33.

27 Lopatin I.V., Akhmadeev Yu.H., Koval N.N., Kovalskiy S.S., Schanin P.M., Yakovlev V.V. // *X International Conference on Modification of Materials with Particle Beams and Plasma Flows*, Tomsk, Russia, September, 19–24, 2010: Proceedings, Tomsk: Publ. House of the IAO SB RAS, 2010, p. 35–38.

Н.Н.Коваль, Ю.Ф.Иванов, О.В.Крысина, В.В.Шугуров, И.В.Лопатин

## Төмен қысымды доғалық разрядта титан нитриді негізінде жасалған көпкомпонентті нанокристалдық бүркемелерді синтездеу

Мақалада иондық-плазмалық қондырғылардың ерекшеліктері мен вакуумдық-доғалық разрядта материалдарды өңдеудің ерекшеліктері қарастырылған. Бүркемелерді қондыруға арналған модификацияландырылған иондық-плазмалық қондырғылардың ерекшеліктері мен басым жақтары сипатталған. Доғалық плазмада генерацияланған газдық және газметалдық плазманың параметрлері келтірілген. Металдық материалдардың бетінің қасиеттерінің өңделуші газразрядты плазманың параметрлерімен байланысы анықталған. Титан нитриді негізінде жасалған көпкомпонентті нанокристалдық бүркемелерді алудың вакуумдық-доғалық плазмалық әдістері сипатталған. Қосымша элементтердің титан нитриді негізінде жасалған бүркемелердің қасиеттері мен құрылымдық-фазалық күйіне әсері көрсетілген.

Н.Н.Коваль, Ю.Ф.Иванов, О.В.Крысина, В.В.Шугуров, И.В.Лопатин

## Синтез многокомпонентных нанокристаллических покрытий на основе нитрида титана в дуговых разрядах низкого давления

В статье рассмотрены особенности ионно-плазменного оборудования и обработки материалов в вакуумных дуговых разрядах. Описаны преимущества и особенности модифицированной ионно-плазменной установки для осаждения покрытий. Представлены результаты измерения параметров генерируемой газовой и газометаллической дуговой плазмы. Выявлены зависимости свойств поверхности металлических материалов от параметров обрабатываемой газоразрядной плазмы. Описан метод вакуумно-дугового плазменно-ассистированного осаждения многокомпонентных нанокристаллических покрытий на основе нитрида титана. Продемонстрировано влияние дополнительного элемента на структурно-фазовое состояние и характеристики нитридтитановых покрытий.

УДК 538.95.405

В.Ч.Лауринас, О.Н.Завацкая, С.А.Гученко

*Карагандинский государственный университет им. Е.А.Букетова (E-mail: exciton@list.ru)*

## Структурно-фазовый состав и свойства композиционных покрытий

Приведены результаты экспериментального исследования фазового состава и структурных параметров композиционных покрытий, полученных в среде азота. Результаты получены на дифрактометре XRD-6000 на CuKα-излучении. С помощью системы наноиндентирования по методу Оливера и Фара с использованием индентера Берковича определена нанотвердость композиционных покрытий и их модуль текучести. На установке Quanta 200 3D проведен элементный анализ по толщине покрытия. Анализ полученных экспериментальных результатов позволил выявить влияние газовой атмосферы на структурные и физико-механические свойства композиционных покрытий.

*Ключевые слова:* плазма, покрытие, нанотвердость, толщина, структура, фазовый состав.

### *Введение*

Одним из способов улучшения свойств поверхности материалов является нанесение композиционных покрытий методом вакуумного ионно-плазменного осаждения [1, 2]. Характерной чертой этих методов является прямое преобразование электрической энергии в энергию технологического воздействия, основанное на структурно-фазовых превращениях в осажденном на поверхности конденсате или в самом поверхностном слое детали, помещенной в вакуумную камеру.